Experiments with 315-Mev Polarized Protons: Proton-Proton and Proton-Neutron Scattering

O. CHAMBERLAIN, E. SEGRÈ, R. D. TRIPP, C. WIEGAND, AND T. YPSILANTIS
Radiation Laboratory and Department of Physics, University of California, Berkeley, California
(Received September 19, 1956)

The polarization in elastic p-p and p-n scattering at 315 Mev has been measured as a function of the scattering angle. The maximum polarization observed in each of these interactions is approximately 40 percent. A similar measurement of the polarization in p-p scattering at 276 Mev is also reported. Triple-scattering experiments have been performed to measure the depolarization $D(\theta)$ and the rotation $R(\theta)$ in the proton-proton interaction. These parameters have been measured for center-of-mass scattering angles ranging from 22 to 80 degrees.

Expressions for the measured quantities in terms of 14-phase shifts of the proton-proton system for $J \leqslant 6$ and $l \leqslant 5$ are included. Two of the phase shifts represent mixing between states of the same total angular momentum J, spin S, and parity. Five sets of phase shifts are reported which satisfy 36 measurements of total cross section, relative differential cross section, polarization, depolarization, rotation, and supplementary conditions imposed by the analysis of information from the reaction $p+p \rightarrow \pi^+ + d$.

I. INTRODUCTION

THE study of the neutron-proton and proton-proton interaction at cyclotron energies ranging from 40 to 450 Mev has been the subject of extensive experimental effort in many laboratories during the past decade. In the experimental program carried on by Segrè, Wiegand, Chamberlain, and collaborators since 1949, the angular distribution and absolute cross sections for p-p and n-p scattering at energies from 40 Mev to 345 Mev have been measured.[1] The theoretical interpretation of these results has generally been attempted by the choice of specific combinations of central and tensor[2–4] or central and spin-orbit[5] Yukawa potentials. The well depth and range parameters, which characterize these potentials, were chosen so that reasonable agreement with the cross-section data was obtained. These potential models have been uniformly unsuccessful in predicting some of the more recent results of the double- and triple-scattering experiments. Such procedures were perhaps warranted in the past, but it now appears that with the more extensive experimental information available a more modest, but sounder, analysis can be made. This involves first the determination of the scattering phase shifts, followed perhaps by their interpretation in terms of meson theory or a potential interaction between nucleons. A review article by Breit and Gluckstern[6] summarizes the experimental and theoretical situation prior to the discovery of polarization effects in high-energy proton-proton scattering by Oxley, Cartwright, and Rouvina.[7]

It may be shown that the information obtainable from high-energy measurements ($E > 100$ Mev) of the angular dependence of the differential cross section is insufficient for the determination of the scattering phase shifts in the nucleon-nucleon system. It then follows that additional independent experimental measurements (e.g., double and triple scattering) are necessary to determine the phase shifts. Yang[8] and Wolfenstein[9] have shown that the highest-order spherical harmonic that may enter into the expression for the nucleon-nucleon differential cross section is $2l_{\max}$, where $l_{\max}$ is the maximum orbital angular momentum of a partial wave that is altered by the interaction. Thus the neutron-proton differential cross section $I_0(\theta)$ can be written as

$$I_0(\theta) = \sum_{n=0}^{2l_{\max}} A_n Y_n^0(\cos\theta), \tag{1}$$

where θ is the center-of-mass scattering angle, Y_n^0 are the normalized Legendre polynomials, and the A_n's are arbitrary coefficients, which can be determined by experiment. Measurements of $I_0(\theta)$ can therefore, in principle, fix $(2l_{\max}+1)$ such coefficients. In a phase-shift description of the n-p elastic scattering we must consider interactions in $(4l_{\max}+2)$ states, since only two interaction states are possible for $l=0$ (i.e., $^1S_0$, $^3S_1$), and four states (one singlet and three triplet) for all higher l values. We must therefore introduce at least $(4l_{\max}+2)$ real phase shifts to describe the scattering. In addition, if l is not conserved (i.e., if tensor forces are present) we must introduce $(l_{\max}-1)$ real parameters (we assume $l_{\max} > 0$) that describe the mixing between states of the same total angular momentum J, spin S, and parity.[10]

[1] Chamberlain, Segrè, and Wiegand, Phys. Rev. **83**, 923 (1951); Hadley, Kelly, Leith, Segrè, Wiegand, and York, Phys. Rev. **75**, 351 (1948); Kelly, Leith, Segrè, and Wiegand, Phys. Rev. **79**, 96 (1950); Chamberlain, Pettengill, Segrè, and Wiegand, Phys. Rev. **93**, 1424 (1954); **95**, 1348 (1954); O. Chamberlain and J. D. Garrison, Phys. Rev. **95**, 1349 (1954); David Fischer and Gerson Goldhaber, Phys. Rev. **95**, 1350 (1954).
[2] R. Christian and E. Hart, Phys. Rev. **77**, 441 (1950).
[3] R. Christian and H. P. Noyes, Phys. Rev. **79**, 85 (1950).
[4] R. Jastrow, Phys. Rev. **79**, 389 (1950).
[5] K. M. Case and A. Pais, Phys. Rev. **80**, 203 (1950).
[6] G. Breit and R. L. Gluckstern, *Annual Reviews of Nuclear Science* (Annual Reviews, Inc., Stanford, 1953), Vol. 2, p. 365.
[7] Oxley, Cartwright, and Rouvina, Phys. Rev. **93**, 806 (1954).
[8] C. N. Yang, Phys. Rev. **74**, 764 (1948).
[9] L. Wolfenstein, Phys. Rev. **75**, 1664 (1949).
[10] J. M. Blatt and L. C. Biedenharn, Revs. Modern Phys. **24**, 258 (1952).

TABLE I. Summary of the experimental parameters obtainable from the angular distribution of the measurements. ($l_{max}>0$.)

	Experiment							
	I_0	P	D	R	A	Total	Phase shifts	
n-p	$2l_{max}+1$	$2l_{max}-1$	$2l_{max}+1$	$2l_{max}+1$	$2l_{max}+1$	$10l_{max}+3$	$5l_{max}+1$	
p-p	$l_{max}+1$	l_{max}	$2l_{max}+1$	$2l_{max}+1$	$2l_{max}+1$	$8l_{max}+4$	$(5/2)l_{max}+(3/2)$	(l_{max} odd)
							$(5/2)l_{max}$	(l_{max} even)

Thus, for a general phase-shift description of the scattering we must introduce a total of $(5l_{max}+1)$ unknown phase shifts. The determination of these from the $(2l_{max}+1)$ experimental numbers (A_n) obtainable from the nuclear cross-section measurements alone is clearly impossible.

Similar results follow for the proton-proton system even though the number of interaction states is reduced by a factor of approximately two because of the Pauli principle. Only one singlet state is allowed for even l and three triplet states for odd l, thus we find $(2l_{max}+1)$ states if l_{max} is even and $(2l_{max}+2)$ states if l_{max} is odd. We must also introduce $(l_{max}-2)/2$ mixing parameters into the phase-shift analysis if l_{max} is even and $(l_{max}-1)/2$ if l_{max} is odd. This leads to $5l_{max}/2$ or $(5l_{max}+3)/2$ parameters in the phase-shift description where the former value is applied if l_{max} is even and the latter if l_{max} is odd. Since we are considering the scattering of identical particles, the differential cross section must be symmetric about $\theta=\pi/2$, and only the even spherical harmonics can enter into Eq. (1). This reduces the number of A_n's obtainable from the p-p cross-section measurements to $(l_{max}+1)$. Consequently, we conclude that the determination of $5l_{max}/2$ or $(5l_{max}+3)/2$ phase shifts from the $(l_{max}+1)$ coefficients (A_n) of the nuclear cross section is impossible.

If we extend these arguments to include the information available from the measurements of polarization $P(\theta)$ and the triple-scattering parameters $D(\theta)$, $R(\theta)$, and $A(\theta)$, first defined by Wolfenstein,[11] the determination of the scattering phase shifts becomes possible. The number of experimental parameters, analogous to the A_n's that could be determined from these measurements is summarized in Table I. In order to obtain with good accuracy the maximum number of parameters shown in Table I, the measurements should be carried out over the entire angular interval $(0<\theta<\pi)$ except in the cases where symmetry conditions apply. For example, in the p-p system we have:

$$I_0(\theta)=I_0(\pi-\theta), \tag{2}$$

$$P(\theta)=-P(\pi-\theta), \tag{3}$$

thus the measurements of the angular distribution of I_0 and P need only be extended over the angular interval $(0\leqslant\theta\leqslant\pi/2)$. Since no such symmetry conditions apply to the triple-scattering parameters[8] D, R, and A, it is desirable that the measurements be extended over the entire angular interval $(0\leqslant\theta\leqslant\pi)$. It will be noted from Table I that the number of experimental parameters is, in all cases, greater than the number of phase shifts needed to describe the scattering problem. Thus, a set of measurements of I_0, P, D, R, and A should overdetermine the nuclear phase shifts. It is necessary that the system be overdetermined if the number of different solutions is to be kept reasonably small.

[11] L. Wolfenstein, Phys. Rev. **96**, 1654 (1954).

II. THEORETICAL

In a previous publication by the present authors[12] (hereafter denoted as I) we have discussed polarization theory and experiments as applied to the scattering of polarized protons from complex nuclei. We assume that the reader is familiar with the content of the theoretical section in I. The main difference in what follows is due to the fact that the target has spin $\frac{1}{2}$ rather than spin zero and to the operation of the Pauli principle in the case of identical particles.

The internal cyclotron proton beam was scattered from Target 1 and acquired a polarization P_1 in the direction $\mathbf{n}_1$ normal to the scattering plane. We recall that the vector $\mathbf{P}$ is identical to $\langle\boldsymbol{\sigma}\rangle$, where $\boldsymbol{\sigma}$ is a vector having as its components the Pauli spin matrices. This beam was subsequently scattered from an unpolarized liquid hydrogen or liquid deuterium target. The experiments described in this paper were designed to determine the intensity and polarization state of the scattered beam as a function of the incident intensity and polarization. A measurement of the relative intensities of the scattered and incident beams suffices to determine the laboratory differential cross section $I_2(\Theta,\Phi)$, where Θ and Φ are laboratory polar and azimuthal scattering angles.[13] In general, $I_2(\Theta,\Phi)$ may depend upon the

[12] Chamberlain, Segrè, Tripp, Wiegand, and Ypsilantis, Phys. Rev. **102**, 1659 (1956).

[13] The laboratory scattering angles Θ, Φ refer to the second scattering. The subscript 2 will be omitted whenever the omission will cause no ambiguity. We choose our coordinate system such that the beam is moving in the $+Z$ direction with the beam polarization vector P_1 in the $+Y$ direction so the usual definition of polar and azimuthal angles in a right-handed coordinate system lead to the relations $z=r\cos\Theta$, $x=r\sin\Theta\cos\Phi$, $y=r\sin\Theta\sin\Phi$. We note that with this convention $\Phi=0$ and $\Phi=\pi$ correspond to left and right scatterings, respectively. The scattering angles θ, ϕ and differential cross section $I_2(\theta,\phi)$ in the center-of-mass system are related to the corresponding quantities in the laboratory system by the equations

$$\tan(\theta/2)=[1+(E_1/2Mc^2)]^{\frac{1}{2}}\tan\Theta,\quad \varphi=\Phi,$$

$$I_2(\theta,\varphi)=\frac{[1+(E_1/2Mc^2)\sin^2\Theta]^2}{4\cos\Theta[1+(E_1/2Mc^2)]}I_2(\Theta,\Phi),$$

where E_1 is the kinetic energy of the incident protons in the laboratory system and Mc^2 is the proton rest energy.

polarization state of the incident beam. The polarization of the scattered beam $\langle\boldsymbol{\sigma}\rangle_2$ may be described in terms of its components in three mutually perpendicular directions. Following Wolfenstein,[8] we consider an orthonormal set of unit vectors $\mathbf{n}_2$, $\mathbf{s}_2$, $\mathbf{k}_2'$ defined by

$$\mathbf{n}_2=\mathbf{k}_2\times\mathbf{k}_2'/|\mathbf{k}_2\times\mathbf{k}_2'|, \tag{4}$$

$$\mathbf{s}_2=\mathbf{n}_2\times\mathbf{k}_2', \tag{5}$$

where $\mathbf{k}_2$ and $\mathbf{k}_2'$ are unit vectors in the incident and outgoing laboratory directions, respectively. It is convenient to define P_i as polarization obtained in the elastic scattering of an unpolarized proton beam from target i, where the direction of P_i is normal to the scattering plane in question. Using this notation, Wolfenstein[8] has shown that

$$I_2(\Theta,\Phi)=I_0(\Theta)[1+\mathbf{P}_1\cdot\mathbf{P}_2]$$
$$=I_0(\Theta)[1+P_1P_2\cos\Phi], \tag{6}$$

$$I_2\langle\boldsymbol{\sigma}\rangle_2\cdot\mathbf{n}_2=I_0(\Theta)[P_2+DP_1\cos\Phi], \tag{7}$$

$$I_2\langle\boldsymbol{\sigma}\rangle_2\cdot\mathbf{s}_2=I_0(\Theta)[A\mathbf{P}_1\cdot\mathbf{k}_2+R\mathbf{P}_1\cdot(\mathbf{n}_2\times\mathbf{k}_2)], \tag{8}$$

$$I_2\langle\boldsymbol{\sigma}\rangle_2\cdot\mathbf{k}_2'=I_0(\Theta)[A'\mathbf{P}_1\cdot\mathbf{k}_2+R'\mathbf{P}_1\cdot(\mathbf{n}_2\times\mathbf{k}_2)], \tag{9}$$

where I_0, P_2, D, A, R, A', R' are functions of the polar scattering angle and the energy E_1 of the incident beam.[13,14] The parameter $I_0(\Theta)$ is the differential scattering cross section for an incident unpolarized beam. The measurement of $I_0(\Theta)$ by the usual single-scattering techniques is straightforward and need not be considered in detail. We cite as reference the measurements of $I_0(\Theta)$ for the p-p system at energies from 120 Mev to 345 Mev by Chamberlain, Segrè, and Wiegand.[1] The measurement of P_2 requires only brief comment. If the beam incident upon the second target (hydrogen or deuterium) is polarized (i.e., $P_1\neq0$), then a measurement of $I_2(\Theta,\Phi=0)$ and $I_2(\Theta,\Phi=\pi)$ suffices to determine $P_2(\Theta)$. We define the asymmetry e_2 in the second scattering by the equation:

$$e_2=\frac{I_2(\Theta,0)-I_2(\Theta,\pi)}{I_2(\Theta,0)+I_2(\Theta,\pi)}. \tag{10}$$

Combining (6) and (10), we find

$$e_2=P_1P_2; \tag{11}$$

thus a knowledge of the incident beam polarization, P_1, and a measurement of the asymmetry in scattering, $e_2(\Theta)$, fixes the value $P_2(\Theta)$. The determination of P_1 has previously been described in I. It entails the measurement of the asymmetry $e_1=P_1P_1$ in a double elastic scattering of protons from beryllium, in which each scattering occurs at the same angle Θ_1.

The determination of the additional Wolfenstein parameters D, A, R, A', and R' requires a third scattering of the beam. Such a scattering from a third target would measure the projection of $\langle\boldsymbol{\sigma}\rangle_2$ in a direction $\mathbf{n}_3$ normal to the third scattering plane. These parameters, however, are related by Eqs. (7), (8), and (9) to the various components of $\langle\boldsymbol{\sigma}\rangle_2$. The observed asymmetry, e_{3n}, in the third scattering process when all three scattering planes coincide is given by

$$e_{3n}=\frac{I_3(+)-I_3(-)}{I_3(+)+I_3(-)}, \tag{12}$$

where $I_3(\pm)$ refers to scattering such that $\mathbf{n}_3$ is parallel to $\pm\mathbf{n}_2$. The differential cross section $I_3(\Theta_3,\Phi_3)$ after the third scattering may be generally written in the form

$$I_3(\Theta_3,\Phi_3)=I_{30}(\Theta)[1+\langle\boldsymbol{\sigma}\rangle_2\cdot P_3\mathbf{n}_3], \tag{13}$$

where I_{30} is the elastic average differential scattering cross section from Target 3. Thus from (12) and (13) we find

$$e_{3n}=\langle\boldsymbol{\sigma}\rangle_2\cdot\mathbf{n}_2P_3. \tag{14}$$

Combining (6), (7), and (14), we obtain, for the plane geometry used in these measurements (e.g., $\Phi_2=0$ or π),

$$e_{3n}=\frac{P_2\pm DP_1}{1\pm P_1P_2}P_3, \tag{15}$$

where the positive (negative) sign is valid for a left (right) second scattering. From Eq. (15) we solve for D in terms of the experimentally measured quantities e_{3n}, $e_3=P_1P_3$, $e_2=P_1P_2$, and $e_1=P_1P_1$, and obtain

$$D=\frac{e_{3n}}{e_3}(e_2\pm1)\mp\frac{e_2}{e_1}. \tag{16}$$

The component $\langle\boldsymbol{\sigma}\rangle_2\cdot\mathbf{s}_2$ may be determined if the third scattering plane is perpendicular to the second. The asymmetry e_{3s} in the third scattering under these conditions is given by

$$e_{3s}=\frac{I_3(+)-I_3(-)}{I_3(+)+I_3(-)}, \tag{17}$$

where $I_3(\pm)$, in this case, refers to scattering such that $\mathbf{n}_3$ is parallel to $\pm\mathbf{s}_2$. Combining (13) and (17), we find

$$e_{3s}=\langle\boldsymbol{\sigma}\rangle_2\cdot\mathbf{s}_2P_3. \tag{18}$$

The asymmetry e_{3s} can be related to A and R through Eqs. (6), (8), and (18). We then obtain

$$e_{3s}=\frac{P_1P_3[A\mathbf{n}_1\cdot\mathbf{k}_2+R\mathbf{n}_1\cdot(\mathbf{n}_2\times\mathbf{k}_2)]}{1+P_1P_2\cos\Phi_2}. \tag{19}$$

The scalar product $\mathbf{n}_1\cdot\mathbf{k}_2$ is nonzero only if the polarization vector of the beam that is incident upon the second target has a component in the direction of motion. The experiments reported in this paper were carried out with a polarized beam which had no longitudinal component

[14] The parameters I_0, P_2, D, A, R, A', R should all have the subscript 2; however, we shall continue to omit this subscript whenever it causes no confusion.

of polarization. Measurements on the parameter $A(\Theta)$ using such beams are clearly impossible, since $\mathbf{n}_1\cdot\mathbf{k}_2=0$. Noting that $\mathbf{n}_1\cdot(\mathbf{n}_2\times\mathbf{k}_2)=\sin\Phi_2$ and solving Eq. (19) for R in terms of the experimentally measured asymmetries, we obtain

$$R=\frac{e_{3s}}{e_3}\frac{1+e_2\cos\Phi_2}{\sin\Phi_2}. \tag{20}$$

Our measurements were carried out at $\Phi_2=270°$; thus Eq. (20) becomes

$$R=-e_{3s}/e_3. \tag{21}$$

An experiment to measure A was recently performed by Simmons in this laboratory. The method used and the results obtained are described in a recently published paper.[15] He utilized an auxiliary magnetic field in the direction $\mathbf{s}_1$, between the first and second scatterers, to rotate the direction of polarization of the incident beam. Owing to the anomalous proton magnetic moment, the average spin vector $\mathbf{P}_1$ precessed about this field with an angular frequency larger than that of the proton motion and resulted in a beam for which $\mathbf{n}_1\cdot\mathbf{k}_2\neq0$.

The quantity $\langle\boldsymbol{\sigma}\rangle_2\cdot\mathbf{k}_2'$ in Eq. (9) represents the component of polarization in the direction of propagation of the twice scattered beam. This component may be most simply measured by the insertion of a magnet between the second and third scatterers with the magnetic field in the direction of $\mathbf{n}_2$. The effect of such a field would be to convert the $\langle\boldsymbol{\sigma}\rangle_2\cdot\mathbf{k}_2'$ component of the polarization to a component at right angles to the direction of motion and so allow the determination of R' in a manner completely analogous to the measurement of R. The remaining parameter A' is not independent, but is related to R, A, and R' by the equation of Wolfenstein.[16] Of the four independent triple-scattering parameters D, R, A, and R', we have measured D and R, while Simmons[15] has obtained a measure of A. The determination of R' was not attempted.

The parameter D may be interpreted as giving the extent to which the second scattering depolarizes an initially polarized beam. From Eqs. (6) to (9), when the first and second scattering planes coincide (i.e., $\mathbf{n}_1\cdot\mathbf{n}_2=\cos\Phi_2=\pm1$), we find that the components of $\langle\boldsymbol{\sigma}\rangle_2$, in the directions $\mathbf{s}_2$ and $\mathbf{k}_2'$ are zero; thus we may write

$$\langle\boldsymbol{\sigma}\rangle_2=\mathbf{n}_2[(P_2\pm DP_1)/(1\pm P_1P_2)]. \tag{22}$$

If the initial beam is completely polarized (i.e., $P_1=1$), then Eq. (22) takes the form

$$\langle\boldsymbol{\sigma}\rangle_2=\pm\mathbf{n}_2[(D\pm P_2)/(1\pm P_2)], \tag{23}$$

from which we see that if $D=1$, the beam after the second scattering remains completely polarized, thus no depolarization of the initial beam occurs in the scattering. The limits on the magnitude of D may be obtained by application of the condition $|\langle\boldsymbol{\sigma}\rangle_2|\leqslant1$ to Eq. (23), which leads to the inequalities

$$-1+2|P_2|\leqslant D\leqslant1. \tag{24}$$

The parameters R and R' describe the rotation of the polarization vector in the plane of the second scattering. If the first and second scattering planes are perpendicular (i.e., $(\mathbf{n}_1\times\mathbf{n}_2)\cdot\mathbf{k}_2=\sin\Phi_2=\pm1$ and $\mathbf{n}_1\cdot\mathbf{n}_2=\cos\Phi_2=0$), the polarization $\langle\boldsymbol{\sigma}\rangle_2$ after the second scattering may be inferred from Eqs. (6) to (9) as

$$\langle\boldsymbol{\sigma}\rangle_2=P_2\mathbf{n}_2\pm P_1(R\mathbf{s}_2+R'\mathbf{k}'_2). \tag{25}$$

From Eq. (25) we note that the component of $\langle\boldsymbol{\sigma}\rangle_2$ normal to the scattering plane is P_2 and is independent of the polarization of the incident beam. The effects due to the polarization of the incident beam are manifest in the scattering plane and may be characterized as a rotation and reduction in magnitude of the initial polarization vector $\mathbf{P}_1$. Equation (25) for a completely polarized initial beam, together with condition $|\langle\boldsymbol{\sigma}\rangle_2|\leqslant1$, leads to the inequality

$$(R^2+R'^2)^{\frac{1}{2}}\leqslant(1-P_2^2)^{\frac{1}{2}}, \tag{26}$$

which restricts the magnitude of the polarization vector in the plane of the scattering. The interpretation of A and A' as rotation parameters follows by identical arguments when $\mathbf{n}_1\cdot\mathbf{k}_2=1$.

III. EXPERIMENTAL TECHNIQUE

A. Proton-Proton Elastic Scattering

The polarization of the beam used for these measurements was $P_1=0.76\pm0.03$, as described in I. The energy and rms energy spread of the beam, for this particular run, were 319 ± 5 Mev, and the beam current was 3×10^5 protons/sec through a rectangular aperture 2 inches high and 0.5 inch wide.

We used as the second scatterer a liquid hydrogen target developed by Cook[17] and subsequently modified by Garrison.[18] The hydrogen container was a 5.6-inch-diameter cylindrical can with cylinder walls of 4-mil stainless steel. The space between the hydrogen-containing cylinder and a concentric 9-inch-diameter Dural cylinder was evacuated to provide insulation from the external environment. The 9-inch-diameter Dural cylinder was constructed with two 5-mil Dural windows along the beam path. The energy lost by the beam, due to ionization, in traversing half of the target was 4 Mev; thus the average energy of the second scattering was 315 Mev. A similar container which was not filled with liquid hydrogen was used for background subtractions.

The protons scattered from the liquid hydrogen target were detected by a three-counter telescope as shown in

[15] James Simmons, Phys. Rev. **104**, 416 (1956).

[16] L. Wolfenstein (private communication). The parameters A, R, A', R' are not all independent. The requirement that the scattering matrix be invariant under time reversal leads to the relation $(A+R')/(A'-R)=\tan(\theta/2)$. See also reference 11.

[17] Leslie Cook, Rev. Sci. Instr. **22**, 1006 (1951).

[18] O. Chamberlain and J. D. Garrison, Phys. Rev. **103**, 1860 (1956).

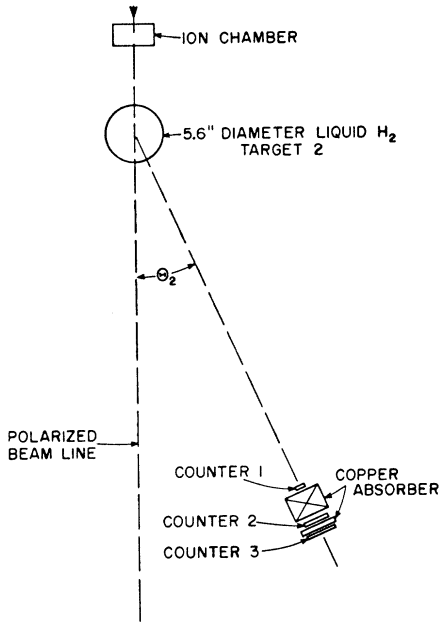

FIG. 1. Scale drawing of liquid hydrogen target 2 and counters used in measurements of polarization in p-p scattering.

Fig. 1. The counters were of standard construction, i.e., polystyrene plastic scintillator viewed by 1P21 photomultiplier tubes. The first counter of the telescope was 1 inch wide and 6 inches high, and served as the solid-angle defining counter. The distance from the center of the hydrogen target to the face of the first counter was 37.5 inches, which corresponds to a solid angle of 4.27×10^{-3} steradian. Variable amounts of copper absorber were inserted between counters to determine the range of the scattered protons. The dimensions of counters 2 and 3 were 2.5 by 8 inches and 3 by 9 inches, respectively. The associated electronic circuits have been previously described in I.

The angular resolution of the system varied with scattering angle Θ_2 because of the non-negligible dimensions of the hydrogen target. Measurements were made at laboratory scattering angles Θ_2 ranging from 10° to 42.5°. At $\Theta_2=10°$ the resolution function is approximately Gaussian with standard deviation of 0.8°. This parameter increased with increasing Θ_2 approximately as $\sin\Theta_2$ so that, at the largest laboratory angle investigated ($\Theta_2=42.5°$), the resolution function had a standard deviation of 2.0°.

The beam current incident upon the hydrogen target was monitored by a 2-inch-deep argon-filled ionization chamber which had been calibrated against a Faraday cup as described in reference 1. An absolute monitor, however, is not essential for the measurement of the polarization. The monitor need only be proportional to the beam current, since the measurement of relative cross sections for left and right scattering suffices to determine the asymmetry.

The center line of the polarized beam in the experimental area was determined by exposure of two x-ray films along the beam path. The scattering apparatus was aligned with respect to the center line, which was preserved in space with the aid of a surveyor's transit. We estimate the angular errors arising from the alignment procedure and other effects related to the apparatus to be 3×10^{-3} radian.

B. Proton-Neutron Elastic Scattering

The polarization in p-n scattering was measured by scattering the polarized proton beam from a liquid deuterium target. For a certain range of angles the scattered protons were detected in coincidence with the recoil neutron. The forward charge-exchange scattering was observed by detection of high-energy neutrons in the forward direction. (The various detection schemes used are discussed in detail later in this section.) The validity of this method rests upon the assumption that the observed polarization due to scattering from the bound neutron in deuterium is equivalent to the polarization in scattering from a free neutron. The symmetry between the neutron and the proton in deuterium allows a convenient test of this assumption. We simultaneously measured the polarization in p-p scattering from the bound proton in deuterium, and compared the results with the measurements of polarization in p-p scattering from liquid hydrogen (described in the preceding section). The polarizations were found to be the same. We interpret this agreement as justification for the use of this method.

Siegal, Hartzler, and Love[19] and Hillman and Stafford[20] have measured the polarization in n-p scattering at 350 Mev and 98 Mev, respectively. These authors observed the asymmetry of the recoil protons when a polarized neutron beam was scattered from liquid hydrogen. Such a technique, although direct and easily interpretable, has some disadvantages because of the difficulties in obtaining highly polarized and intense neutron beams.

In order to increase the polarized beam current available in the experimental area, we used a 2-inch-diameter collimator. The beam current so obtained was approximately 10^6 protons/sec. The beam polarization was $P_1=0.69\pm0.05$, and the measured energy and rms energy spread was 315 ± 12 Mev. We monitored the beam with an argon-filled ionization chamber as previously described.

The liquid deuterium target was constructed by Roscoe Byrns of this laboratory. A detailed description of a similar deuterium target has been given by Nagle.[21] The deuterium-containing cylinder was 8 inches in length and 4 inches in diameter, oriented so that the axis of the cylinder coincided with the beam line. Ends of the cylinder were of 4-mil brass and the cylinder walls were $\frac{1}{32}$-inch brass. The proton beam, on entering or

[19] Siegal, Hartzler, and Love, Phys. Rev. **101**, 836 (1956).
[20] E. Hillman and G. H. Stafford, Nuovo cimento **3**, 633 (1956).
[21] D. E. Nagle, Phys. Rev. **97**, 480 (1955).

leaving the deuterium volume, traversed a 4-mil Dural and a 4-mil brass window. The energy loss in traversing half of the target was 5 Mev, thus the average scattering energy was 310 Mev. The liquid deuterium could be removed from the target cylinder whenever necessary for the study of the background scattering from the target walls. The scattering from the liquid deuterium was determined by subtraction of the target-empty scattering from the scattering when the target was filled.

A scale drawing of the neutron counter and the geometrical arrangement of the apparatus is shown in Fig. 2. The neutron counter consisted of six counters (Nos. 1 through 6), each 3 by 3 by 0.25 inches, and three shield counters A_1, A_2, A_3 with dimensions 5 by 4 by 0.5, 10 by 4 by 0.5, and 10 by 4 by 0.5 inches, respectively. Signals from the three guard counters were combined to give a signal A. Slabs of polyethylene converter (or carbon of the same stopping power) could be inserted between counters A_1, 1, 2, 3, and 4 as indicated in Fig. 2. Copper absorbers of the same stopping power as the polyethylene converter could be inserted between counters 4 and 5 or 5 and 6.

Large-angle charge-exchange scattering gives rise to a low-energy proton at large angles with the conjugate high-energy neutron in the forward direction. In this case, a coincidence counting arrangement to detect both the neutron and the conjugate proton is unfeasible, as the proton has insufficient energy to leave the target. We therefore utilized the energy discrimination provided by the neutron counter to observe the polarization in this angular interval. For laboratory scattering angles Θ_n between 7° and 33°, the detection scheme was such that only neutrons with energy greater than 112 Mev were counted by the neutron counter. The laboratory scattering angle Θ_n refers to the angle the neutron in the final state makes with the direction of the incident beam. The observed asymmetries, however, are given as a function of the angle Θ, which refers to the angle the proton in the final state makes with the incident-beam direction. The relativistic kinematic relation between these angles is approximately

$$\Theta+\Theta_n=\frac{\pi}{2}-\frac{E_1}{4Mc^2}\sin(2\Theta), \tag{27}$$

where E_1 is the average scattering energy (310 Mev) and M is the proton rest mass. The relativistic term in Eq. (27) reduces the included angle between neutron and proton at this energy, by a maximum of 5% from the nonrelativistic value $\pi/2$.

Signals from counters 1 through 6 could be added together in different ways depending upon the energy discrimination desired. Signals a, b, and c were obtained by adding the output signals from counters 1 and 4, 2 and 5, and 3 and 6, respectively. A coincidence between signals a, b, and c in anticoincidence with the guard signal A we interpret as a neutron of energy greater than

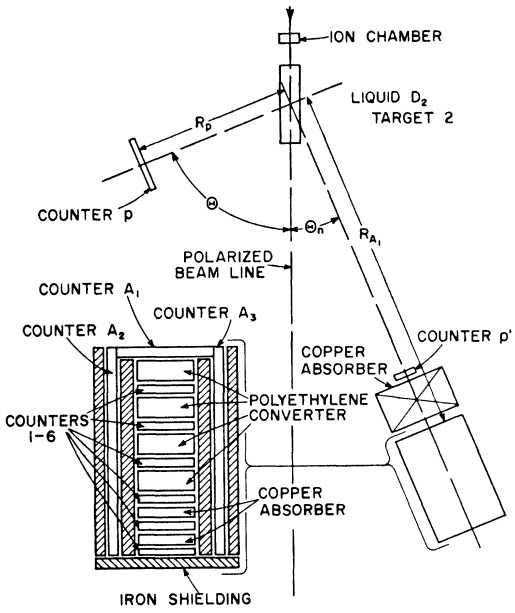

FIG. 2. Scale drawing of liquid deuterium cylinder and counters used in the measurement of polarization in p-n scattering.

112 Mev. The combination of signals $abc\bar{A}$ (read abc not A) could occur when a neutron passed through A_1 without counting and subsequently suffered a charge-exchange scattering in one of the polyethylene slabs or in one of the counters 1 through 4. The proton resulting from such a collision must have sufficient energy to traverse a minimum of two polyethylene slabs (or copper of the same stopping power), and any three of the counters 1 through 6. The polyethylene slabs had stopping power equivalent to 5.7 g/cm² copper. Each of the counters 1 through 6 had stopping power equivalent to 1.0 g/cm² copper, thus the event $abc\bar{A}$ requires that the knock-on proton have a minimum range of 14.4 g/cm² copper which corresponds to a kinetic energy of 112 Mev. For the measurements in this angular interval, copper absorber in excess of that necessary to stop 310-Mev protons was placed before counter A_1 in an attempt to eliminate the primary charge particle flux incident upon counter A_1. This minimized the number of spurious events due to protons from the deuterium target against which the anticoincidence circuit should discriminate.

A second detection scheme was used for scattering angles Θ_n between 30° and 47°. In this angular region the conjugate protons have sufficient energy to leave the target system. A coincidence between the neutron signal and the signal from counter p placed at the conjugate angle Θ was required in this angular interval. Dimensions of the scintillator in counter p were 5.62 by 4.12 by 0.5 inches. Energy discrimination in the neutron counter was not essential because the requirement of an additional coincidence in counter p discriminated against the ambient neutron background. An increased efficiency of

the neutron counter was obtained by adding signals from counters 1, 3, and 5 to give signal d and 2, 4 and 6 to give signal e. The minimum neutron energy necessary for the coincidence dep was approximately 75 Mev. In this angular interval the coincidence dep in anticoincidence with the guard signal A we interpreted as a p-n scattering event. An additional counter p' was placed in front of counter A_1. Coincidences pp' correspond to proton-proton scattering from the bound proton in deuterium. The measurements of the coincidences $dep\bar{A}$ and pp' were carried out simultaneously.

The remaining range of scattering angles Θ_n between 47° and 79° were observed by using essentially the same detection scheme as outlined in the previous paragraph. A modification was made to further increase the neutron counter efficiency. Signals from counters 1 through 6 were added to give signal f. The event $fp\bar{A}$ we interpret as a p-n scattering in this angular interval.

Measurement of the absolute efficiency of the neutron detector for the determination of the polarization was unnecessary. No attempt was made to measure this parameter.

The lineup procedure used was identical to that described for the proton-proton polarization measurements in the preceding section.

C. Triple Scattering—Depolarization and Rotation of the Polarization Vector in p-p Scattering

The objective of these experiments was to measure the change of the polarization state when a polarized proton beam was scattered from an unpolarized hydrogen target. Such a measurement requires three scattering processes. The first scattering produces the polarized proton beam that is subsequently scattered from liquid hydrogen (target 2). The polarization state of the protons scattered from the second target through an angle (Θ_2,Φ_2) is determined by a measurement of the asymmetry in the third scattering.

The polarized proton beam was incident upon the liquid hydrogen second target. A scattered beam was defined by a coincidence between a pair of counters (called 1 and 2) at the angle (Θ_2,Φ_2) of interest. We measure a polarization component of the beam by scattering from a third target of carbon or beryllium through an angle (Θ_3,Φ_3). A typical arrangement of the counters and targets used in the measurement of the depolarization parameter D is shown in Fig. 3. A triple scattering event was defined by a coincidence between counters 1, 2, 3, and 4. With this system protons scattered directly from the hydrogen target into counters 3 and 4 contributed only to the accidental events. Coincidences between counters 3 and 4 alone were approximately one thousand times as numerous as the coincidences 1–2–3–4; thus the discrimination provided by counters 1 and 2 was indispensable. In spite of the relatively high 3–4 coincidence rate the accidental 1–2–3–4 coincidences were less than 10% of the total 1–2–3–4 coincidence counting rate.

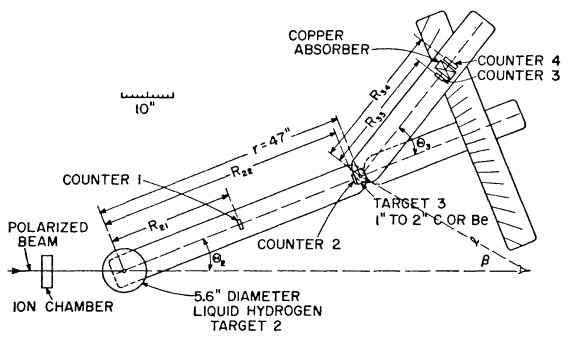

FIG. 3. Scale drawing of triple-scattering apparatus and counters used in the measurement of the depolarization parameter $D(\Theta_2)$. For the geometry shown, the second scattering occurs at $\Phi_2=0°$. Target 1, a one-inch beryllium target inside the cyclotron, is not shown in this figure.

The energy spread of the beam defined by 1–2 coincidences is determined by the angular resolution of the apparatus (see Fig. 3) and the energy spread of the incident polarized beam. The kinetic energy E_2 after the second scattering depends upon the incident energy E_1 and the scattering angle Θ_2. The relativistic relation between these quantities is

$$E_2=E_1\cos^2\Theta_2\Big/\left(1+\frac{E_1}{2Mc^2}\sin^2\Theta_2\right), \qquad (28)$$

where Mc^2 is the proton rest energy. From Eq. (28) we note that the proton energy at the inner edge of Counter 2 will be greater than the proton energy at the outer edge of this counter. The magnitude of the energy spread is given, to a good approximation, by

$$\Delta E_2=E_1\sin(2\Theta_2)\Delta\Theta_2, \qquad (29)$$

where $\Delta\Theta_2$ is the angular width of counter 2. This correlation between energy and position across the face of counter 2 may induce false asymmetries in the third scattering if the absorber between counters 3 and 4 is excessive.

The range of the twice scattered beam at angle (Θ_2,Φ_2) was determined by setting $\Theta_3=0°$ and measuring the 1–2–3–4 coincidence rate as a function of the absorber between counters 3 and 4. The range curve obtained at a given scattering angle (Θ_2,Φ_2) was used as the basis for choice of the final absorber value between counters 3 and 4. In view of the large polarizations which have been observed in the elastic scattering of protons from complex nuclei, the absorber between counters 3 and 4 was adjusted so that highly inelastic scatterings from the third target would not be accepted. The absorber value so chosen was always substantially smaller than the mean range of the twice scattered beam. This precluded the possibility of false asymmetries arising from the energy correlation with position across the beam.

The beam profile of the twice scattered beam was observed by measuring the 1–2–3–4 coincidence rate as a function of the third scattering angle Θ_3. With the absorber between counters 3 and 4 chosen as described in the previous paragraph the beam profile was symmetric about $\Theta_3=0°$ and is shown by curve A in Fig. 4. When the absorber between counters 3 and 4 was increased to a value near the mean range of the twice scattered beam the beam profile had its center of gravity shifted toward smaller Θ_2 angles. An example of such a beam profile is shown by curve B in Fig. 4. We verified, in all cases, that the beam profile at a given scattering angle (Θ_2,Φ_2) was symmetric about $\Theta_3=0°$, thus eliminating the possibility of false asymmetries

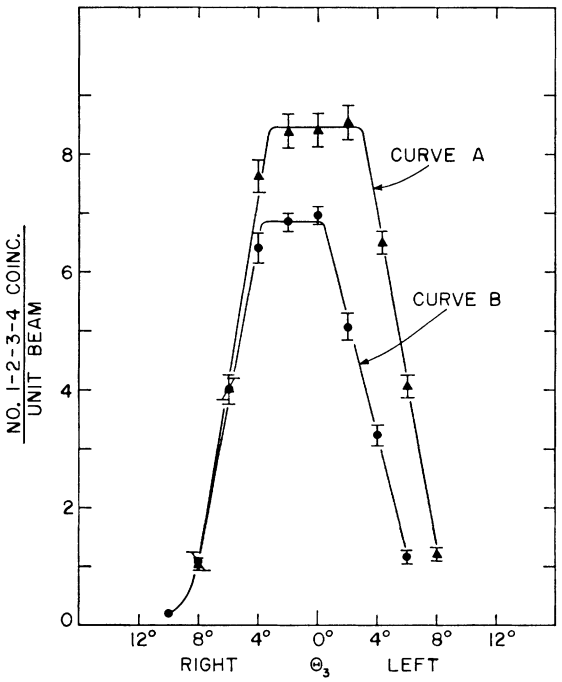

FIG. 4. Beam profile of twice-scattered beam. Curve A was obtained when the absorber between counters 3 and 4 was chosen as described in the text. Curve B was obtained when the 3–4 absorber was excessive.

caused by a choice of the 3–4 absorber which was excessive.

The analyzing angle Θ_3 was chosen by extending the measurements of the beam profile to large scattering angles. A characteristic beam profile, plotted on a logarithmic scale, is shown in Fig. 5. In the angular interval between 4° and 8° the counting rate is an extremely rapidly varying function of scattering angle Θ_3 and depends mainly on multiple Coulomb scattering from the third target. At larger angles the counting rate decreases more slowly with a slope characteristic of nuclear elastic scattering from the carbon or beryllium third target. We chose the analyzing angle Θ_3 outside the region of the Coulomb scattering and safely into the

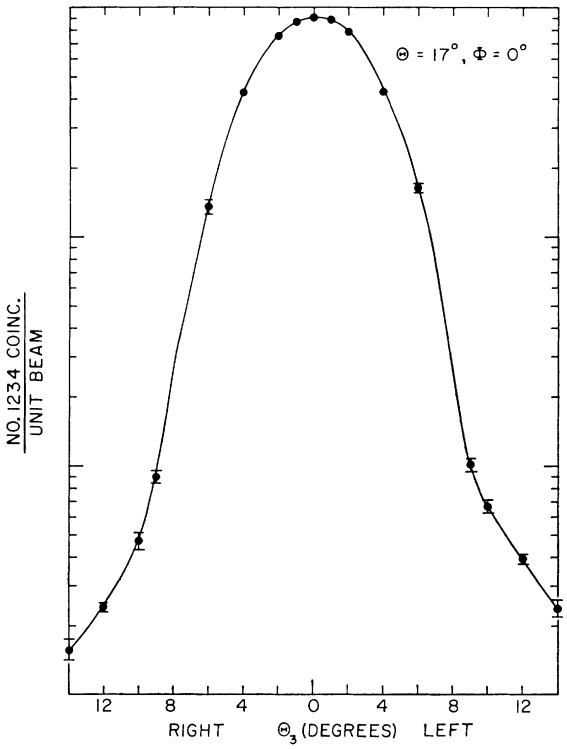

FIG. 5. Beam profile of the twice scattered beam at $(\Theta=17°, \Phi=0°)$.

region of the nuclear scattering. In all cases the analyzing angle so chosen was inside the region of the first elastic scattering diffraction minimum, thus insuring that the scattering events observed were primarily elastic.

Calibration of the analyzing power, $e_3=P_1P_3$, of the third scattering was accomplished by removing the hydrogen target from the beam and setting $\Theta_2=\Theta_3=0°$ (i.e., all counters directly in the beam line). The polarized proton beam was degraded in energy by the insertion of a calculated amount of uranium absorber at the position of the second target. The uranium degrader served also to multiple scatter the degraded polarized beam so that coincidences between counters 1 and 2 defined a beam with angular divergence similar to the divergence of the beam scattered from the liquid hydrogen target. The beam current entering the experimental area was reduced to approximately 10^3 protons/sec by reducing the cyclotron filament arc voltage. This method has the advantage that all the cyclotron parameters (magnetic field, etc.) which might have affected the polarization of the incident beam remained unchanged. With the degrader at the second target position a range curve of the beam, defined by coincidences between counters 1 and 2, was obtained by varying the absorber between counters 3 and 4 and counting the 1–2–3–4 coincidences with the 1–2 coincidence rate as the beam monitor. Calibrations of the analyzing power were

TABLE II. Polarization in proton-proton elastic scattering at 315 Mev.

θ	$e_H = P_1 P_H$	$I_0(10^{-27}$ cm^2/sterad)	P_H
21.6°	0.232±0.015	3.64±0.06	0.305±0.023
32.3°	0.287±0.017	3.60±0.07	0.378±0.027
42.9°	0.288±0.010	3.75±0.05	0.379±0.020
53.4°	0.230±0.017	3.68±0.07	0.303±0.025
63.9°	0.191±0.019	3.65±0.07	0.251±0.027
76.2°	0.108±0.019	3.70±0.07	0.142±0.025
89.4°	−0.004±0.013	3.60±0.07	−0.005±0.016

TABLE III. Polarization in proton-proton elastic scattering at 276 Mev.

θ	$e_H = P_1 P_H$	P_H
19.3°	0.214±0.019	0.314±0.036
27.8°	0.217±0.022	0.324±0.041
32.0°	0.227±0.009	0.329±0.028
49.9°	0.198±0.011	0.295±0.027
63.4°	0.168±0.013	0.251±0.027
76.8°	0.082±0.013	0.122±0.021
90.0°	0.029±0.014	0.044±0.019

carried out after every measurement of e_{3n} at a given angle (Θ_2,Φ_2). It was necessary that the range curve for the calibration measurement match as closely as possible the range curve of the beam scattered at angle (Θ_2,Φ_2) from the liquid hydrogen second target. To this end small adjustments were made on the thickness of the beam degrader until the two range curves were matched. The measurement of the analyzing power, e_3, was made at the angle Θ_3 of interest with the same absorber between counters 3 and 4 as was used in the measurements of e_{3n} at the given angle (Θ_2,Φ_2). A systematic error in the calibration would be introduced if the polarization of the incident proton beam were changed by the energy degradation process. Calculations carried out by Wolfenstein[9] indicate depolarization effects in the passage of charged particles through matter are negligible. This conclusion has been confirmed experimentally.[22]

IV. EXPERIMENTAL RESULTS

A. Proton-Proton Elastic Scattering

The data obtained are summarized in Table II and the dependence of the polarization on center-of-mass scattering angle, θ, is shown in Fig. 6. Measurements of the average differential cross section $I_0=[I(\theta,0)-I(\theta,\pi)]/2$ are also included. The errors given for e_H and I_0 are standard deviations due to counting statistics only. As a consequence of the weak dependence of $I_0(\Theta)$ upon Θ (i.e., $I_0(\Theta)\propto\cos\Theta$), the systematic errors in the measurement of e_H are completely negligible compared to the counting errors. Systematic effects in the measurements of I_0 due to extrapolation of counter plateaus to zero bias, absolute calibration of ion chamber, and attenuation correction due to absorber in counter telescope lead to an estimated 10% systematic error to be superimposed upon the statistical errors given in Table II. The measurements of $I_0(\theta)$ by Chamberlain, Segrè, and Wiegand[1] are statistically more reliable and should be used in preference to the measurements of $I_0(\theta)$ reported here. The cross section measurements shown in Table II were obtained as a by-product of the experiment which was primarily designed to measure the polarization. The value of P_H was obtained from the corresponding value of e_H through the relation $P_H=e_H/P_1$. The value of $P_1=0.76\pm0.03$ includes all known errors in beam calibration. In arriving at the errors for P_H quoted in Table II the 4% error arising from the measurement of P_1 has been included. In addition to the polarization measurements reported here, we have previously published some results of

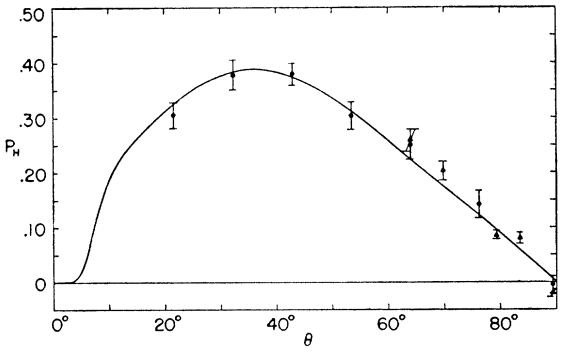

FIG. 6. Polarization in p-p elastic scattering at 315 Mev. The triangle points represent the polarization observed in p-p scattering from deuterium. The curve shown is from phase shift solution 4 of the text.

[22] Heiberg, Kruse, Marshall, Marshall, and Solmitz, Phys. Rev. **97**, 250 (1955).

TABLE IV. Polarization in proton-neutron elastic scattering in deuterium at 310 Mev.

θ	Coincidence	e	P_n
21.6	pA_1	0.319±0.056	0.462±0.081
32.3	pA_1	0.278±0.033	0.403±0.048
42.9	$fp\bar{A}$	0.263±0.025	0.382±0.036
53.4	$fp\bar{A}$	0.155±0.019	0.225±0.028
63.9	$fp\bar{A}$	0.109±0.021	0.158±0.030
74.2	$fp\bar{A}$	−0.008±0.021	−0.012±0.030
82.3	$fp\bar{A}$	−0.062±0.019	−0.090±0.028
82.3	$dep\bar{A}$	−0.087±0.023	−0.126±0.033
90.6	$dep\bar{A}$	−0.067±0.022	−0.197±0.032
100.7	$dep\bar{A}$	−0.164±0.021	−0.238±0.030
109.9	$abc\bar{A}$	−0.172±0.050	−0.249±0.072
110.2	$dep\bar{A}$	−0.180±0.021	−0.261±0.030
116.1	$dep\bar{A}$	−0.157±0.022	−0.228±0.032
121.3	$abc\bar{A}$	−0.176±0.030	−0.255±0.043
130.8	$abc\bar{A}$	−0.153±0.027	−0.222±0.039
137.3	$abc\bar{A}$	−0.136±0.018	−0.197±0.026
147.7	$abc\bar{A}$	−0.139±0.020	−0.202±0.029
158.4	$abc\bar{A}$	−0.051±0.016	−0.074±0.023
164.9	$abc\bar{A}$	−0.016±0.024	−0.023±0.035

TABLE V. Depolarization in proton-proton elastic scattering at 310 Mev.

θ	Target 3	Θ_3	$e_3=P_1P_3$	$e_{3n}(\phi=0)$	$e_{3n}(\phi=\pi)$	D (average)
23.1°	2-in. C	12.0°	0.472±0.014	0.275±0.041	0.135±0.055	0.245±0.079
25.8°	2-in. Be	12.7°	0.490±0.014	0.349±0.031	0.155±0.034	0.299±0.055
36.5°	2-in. C	12.0°	0.466±0.014	0.357±0.043	0.048±0.055	0.456±0.081
52.0°	2-in. Be	12.8°	0.471±0.012	0.368±0.041	−0.042±0.030	0.533±0.060
65.2°	2-in. Be	15.1°	0.468±0.012	0.321±0.029	−0.100±0.033	0.503±0.048
80.5°	1-in. Be	20.5°	0.545±0.024	0.315±0.026	...	0.472±0.063

earlier measurements of polarization in p-p scattering.[23] At the time of publication of these results, the polarization of the incident 280-Mev proton beam was undetermined. Therefore only the measured asymmetries were reported. The polarization of this beam was subsequently determined to be $P_1=0.67\pm0.05$. In Table III are listed the asymmetries and the derived value of the polarization at an average scattering energy of 276 Mev. The errors listed for the polarization in Table III include the error in the incident beam polarization. Similar measurements have been made at 130 Mev by Dickson and Salter,[24] at 170 Mev by Fischer and Baldwin,[25] at 310 Mev by Marshall, Marshall, and DeCarvalho,[26] at 415 Mev by Kane, Stallwood, Sutton, Fields, and Fox,[27] and at 439 Mev by DeCarvalho, Heiberg, Marshall, and Marshall.[28] More recently, Taylor[29] has reported polarization measurements at 142 Mev.

B. Proton-Neutron Elastic Scattering

The observed asymmetries in p-n scattering from deuterium are listed in Table IV along with the detection schemes used at the various angles. The average energy of the scattering was 310 Mev and the incident beam polarization was $P_1=0.69\pm0.05$. Errors listed for p-n polarization are standard deviations due to counting statistics only. An additional 7% error arising from the uncertainty in the incident beam polarization should be superimposed on the counting statistics; however, the relative angular distribution of the polarization function is not affected by this error. The data of Table IV have been plotted in Fig. 7. A preliminary account of these measurements has been previously reported in this journal.[30]

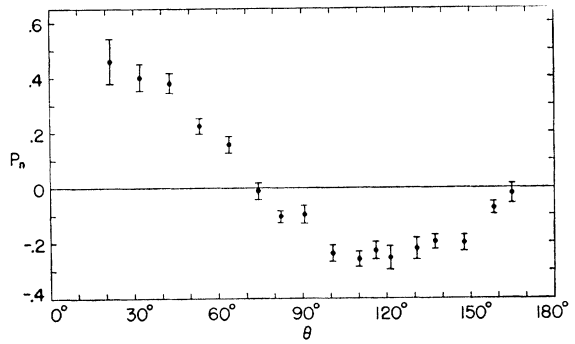

FIG. 7. Polarization in p-n elastic scattering at 310 Mev in deuterium.

C. Depolarization in Proton-Proton Elastic Scattering

The depolarization parameter D was determined at six laboratory angles ranging from 10.7° to 38.1° at an average energy of 310 Mev. The results of these measurements are summarized in Table V and plotted as a function of the center-of-mass scattering angle in Fig. 8. The errors listed in Table V include the contributions from the errors in the measurements of e_1, e_2, e_3 as well as e_{3n}. At five of the six scattering angles θ, the measurements were made at $\varphi=0$ and $\varphi=\pi$ and the values of D were obtained through the use of Eq. (16). Space limitations in the experimental area prevented the measurement of $e_{3n}(\varphi=\pi)$ at the sixth scattering angle $\theta=80.5°$. The values of D obtained at $\varphi=0$ and $\varphi=\pi$ were combined statistically and the resulting average value of D for the two measurements is listed in Table V.

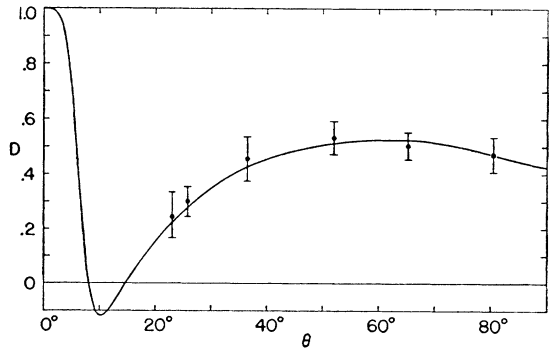

FIG. 8. Depolarization in p-p elastic scattering at 310 Mev. The curve shown is from phase shift solution 4 of the text.

[23] Chamberlain, Segrè, Tripp, Wiegand, and Ypsilantis, Phys. Rev. **93**, 1430 (1954).
[24] J. M. Dickson and D. C. Salter, Nature **173**, 946 (1954).
[25] D. Fischer and J. Baldwin, Phys. Rev. **100**, 1445 (1955).
[26] Marshall, Marshall, and DeCarvalho, Phys. Rev. **93**, 1431 (1954).
[27] Kane, Stallwood, Sutton, Fields, and Fox, Phys. Rev. **95**, 1694 (1954).
[28] De Carvalho, Heiberg, Marshall, and Marshall, Phys. Rev. **94**, 1796 (1954).
[29] A. E. Taylor, *Proceedings of the Sixth Annual Rochester Conference on High-Energy Physics, April 1956* (Interscience Publishers, Inc., New York, 1956).
[30] Chamberlain, Donaldson, Segrè, Tripp, Wiegand, and Ypsilantis, Phys. Rev. **95**, 850 (1954).

D. Rotation of the Polarization Vector

Measurements of the rotation parameter R were obtained at six laboratory scattering angles ranging from 10.4° to 38.1° at an average energy of 310 Mev. The azimuthal angle of the second scattering was $\varphi=3\pi/2$, which corresponds to the downward direction. The determination of R at $\varphi=\pi/2$ was not attempted because of instrumental limitations. In Table VI are listed the pertinent experimental measurements of e_3 and e_{3s} necessary for the evaluation of R according to Eq. (21). The errors in the determination of R include the contribution from the error in e_3 as well as e_{3s}. In Fig. 9 the dependance of R on the center-of-mass scattering angle θ is exhibited. The initial results of both the D and R measurements have been reported in a previous publication.[31]

V. INTERPRETATION OF THE DATA

In this and previous work,[1,15] information on the p-p system at a laboratory scattering energy near 310 Mev has been accumulated. The measurements include the total cross section σ_{tot}, the differential cross section I_0, polarization P, and the triple scattering parameters D, R, and A. Following the treatment of Wolfenstein,[11] we may express the observables in terms of the parameters of the M matrix:

$$M=BS+C(\boldsymbol{\sigma}+\boldsymbol{\sigma}_t)\cdot\mathbf{n}+\tfrac{1}{2}G(\boldsymbol{\sigma}\cdot\mathbf{K}\boldsymbol{\sigma}_t\cdot\mathbf{K}+\boldsymbol{\sigma}\cdot\mathbf{P}\boldsymbol{\sigma}_t\cdot\mathbf{P})T +\tfrac{1}{2}H(\boldsymbol{\sigma}\cdot\mathbf{K}\boldsymbol{\sigma}_t\cdot\mathbf{K}-\boldsymbol{\sigma}\cdot\mathbf{P}\boldsymbol{\sigma}_t\cdot\mathbf{P})T+N\boldsymbol{\sigma}\cdot\mathbf{n}\boldsymbol{\sigma}_t\cdot\mathbf{n}T, \quad (30)$$

where $\boldsymbol{\sigma}$ and $\boldsymbol{\sigma}_t$ are the Pauli spin operators corresponding to the incident and target protons. In Eq. (30), $\mathbf{K}$ and $\mathbf{P}$ are unit vectors in the direction $\mathbf{p}'-\mathbf{p}$ and $\mathbf{p}'+\mathbf{p}$, respectively, where $\mathbf{p}'$ and $\mathbf{p}$ are the outgoing and incident momenta in the center-of-mass system. The vector $\mathbf{n}$ is a unit vector normal to the scattering plane and T and S are the triplet and singlet projection operators. The parameters B, C, G, H, and N are complex scalar functions of the center-of-mass scattering angle θ and the energy. Parity considerations show that B, H, and $C/\sin\theta$ are even functions of $\cos\theta$ and G and N are odd functions of $\cos\theta$. The scattering is completely described by the M matrix and the experimental observables are related explicitly to the parameters B, C, G, H, and N, by the following equations:

$$\begin{aligned}
I_0&=\tfrac{1}{4}|B|^2+2|C|^2+\tfrac{1}{4}|G-N|^2+\tfrac{1}{2}|N|^2+\tfrac{1}{2}|H|^2,\\
I_0P&=2\,\mathrm{Re}C^*N,\\
I_0(1-D)&=\tfrac{1}{4}|G-N-B|^2+|H|^2,\\
I_0R&=\tfrac{1}{2}\,\mathrm{Re}[(G-N)^*(N+H)+B^*(N-H)]\times\cos(\theta/2)+\mathrm{Im}[C^*(B+G-N)]\times\sin(\theta/2),\\
I_0A&=-\tfrac{1}{2}\,\mathrm{Re}[(G-N)^*(N+H)+B^*(N-H)]\times\sin(\theta/2)+\mathrm{Im}[C^*(B+G-N)]\times\cos(\theta/2).
\end{aligned} \quad (31)$$

The connection between the observables and phase shifts for the p-p system has been obtained in an accompanying paper.[32] We may conveniently summarize the results of this analysis by writing the relations between the Wolfenstein parameters B, C, G, H, and N and the phase shifts. In the singlet state of two protons the spin angular momentum is zero and the total angular momentum $j=l$, where l is the orbital angular momentum of a given partial wave. Similarly for triplet states $j=l$ or $l\pm1$. We denote singlet phase shifts as δ_l and the triplet phase shifts by δ_{lj}. In this analysis we have considered the scattering in all states with $j\leqslant6$ and $l\leqslant5$, compatible with the Pauli principle; i.e., $^1S_0$, $^3P_0$, $^3P_1$, $^3P_2$, $^1D_2$, $^3F_2$, $^3F_3$, $^3F_4$, $^1G_4$, $^3H_4$, $^3H_5$, and $^3H_6$. Since l is not known to be a constant of the motion, we must also allow for the possibility of mixing between states with the same spin, total angular momentum, and parity, these quantities being exact constants of the motion for our system. For the states under consideration, mixing may occur between $^3P_2$ and $^3F_2$ states and also between $^3F_4$ and $^3H_4$ states. We utilize the analysis and notation of Blatt and Biedenharn[10] in which the mixing of two states of total angular momentum j is described by a parameter ϵ_j. Thus the mixing between $^3P_2$ and $^3F_2$ is described by ϵ_2 and between $^3F_4$ and $^3H_4$ by ϵ_4. The significance of these parameters is more fully described in reference 32. In accord with the notation of

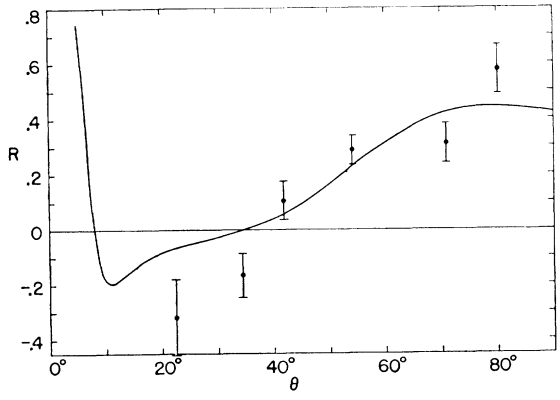

FIG. 9. Rotation of polarization vector in p-p elastic scattering at 310 Mev. The curve shown is from phase shift solution 4 of the text.

TABLE VI. Rotation of polarization vector in proton-proton elastic scattering at 310 Mev.

θ	Target 3	Θ_3	$e_3=P_1P_3$	$e_{3s}(\phi=3\pi/2)$	R
22.4°	1.5-in. C	13.7°	0.438±0.023	0.142±0.060	−0.324±0.139
34.4°	1.75-in. C	12.4°	0.479±0.017	0.080±0.038	−0.167±0.080
41.8°	1.5-in. C	13.7°	0.517±0.016	−0.054±0.037	0.104±0.071
54.1°	1.5-in. C	13.9°	0.491±0.017	−0.141±0.025	0.287±0.052
70.9°	1.5-in. C	15.1°	0.520±0.023	−0.161±0.036	0.310±0.072
80.1°	1.0-in. Be	20.5°	0.501±0.024	−0.289±0.041	0.576±0.087

[31] Ypsilantis, Wiegand, Tripp, Segrè, and Chamberlain, Phys. Rev. **98**, 840 (1955).

[32] Stapp, Ypsilantis, and Metropolis, following paper, Phys. Rev. **105**, 302 (1957).

reference 32, we define the quantities

$$\alpha_l = e^{2i\delta_l} - e^{2i\Phi_l},$$
$$\alpha_{lj} = e^{2i\delta_{lj}} - e^{2i\Phi_l}, \tag{32}$$
$$\alpha^j = \tfrac{1}{2}\sin(2\epsilon_j)(e^{2i\delta_{j\mp1,j}} - e^{2i\delta_{j\pm1,j}}),$$

where

$$\Phi_l \equiv \eta_l - \eta_0 = \sum_{x=1}^{l} \arctan\binom{n}{x}, \tag{33}$$

and $n = e^2/\hbar v$, where v is the laboratory velocity of the incident proton.

The results of the phase shift analysis, including nonrelativistic Coulomb effects, are summarized in the following equations:

$$B = f_C(\theta) + f_C(\pi-\theta) + \frac{1}{8ik}\{[8\alpha_0 - 20\alpha_2 + 27\alpha_4] + [60\alpha_2 - 270\alpha_4]\cos^2\theta + 315\alpha_4\cos^4\theta\}, \tag{34}$$

$$C = -\frac{\sin\theta}{64k}\{[16\alpha_{10} + 24\alpha_{11} - 40\alpha_{12} - 40\alpha_{32} - 14\alpha_{33} + 54\alpha_{34} + 54\alpha_{54} + 11\alpha_{55} - 65\alpha_{56}] + [200\alpha_{32} + 70\alpha_{33} - 270\alpha_{34} - 756\alpha_{54} - 154\alpha_{55} + 910\alpha_{56}]\cos^2\theta + [1134\alpha_{54} + 231\alpha_{55} - 1365\alpha_{56}]\cos^4\theta\}, \tag{35}$$

$$H = \frac{1}{32ik}\{[16\alpha_{10} - 24\alpha_{11} + 8\alpha_{12} - 8\alpha_{32} + 14\alpha_{33} - 6\alpha_{34} + 6\alpha_{54} - 11\alpha_{55} + 5\alpha_{56} - (32\sqrt{6})\alpha^2 + (48\sqrt{5})\alpha^4] + [40\alpha_{32} - 70\alpha_{33} + 30\alpha_{34} - 84\alpha_{54} + 154\alpha_{55} - 140\alpha_{56} + (80\sqrt{6})\alpha^2 - (456\sqrt{5})\alpha^4]\cos^2\theta + [126\alpha_{54} - 231\alpha_{55} + 105\alpha_{56} + (504\sqrt{5})\alpha^4]\cos^4\theta\}, \tag{36}$$

$$N = f_C(\theta) - f_C(\pi-\theta) + \frac{1}{32ik}\{[16\alpha_{10} + 24\alpha_{11} + 56\alpha_{12} - 136\alpha_{32} - 14\alpha_{33} - 186\alpha_{34} + 294\alpha_{54} + 11\alpha_{55} + 355\alpha_{56} + (16\sqrt{6})\alpha^2 - (24\sqrt{5})\alpha^4]\cos\theta + [200\alpha_{32} + 70\alpha_{33} + 290\alpha_{34} - 1316\alpha_{54} - 154\alpha_{55} - 1610\alpha_{56} + (56\sqrt{5})\alpha^4]\cos^3\theta + [2016\alpha_{54} + 231\alpha_{55} + 1407\alpha_{56}]\cos^5\theta\}, \tag{37}$$

$$G - N = f_C(\theta) - f_C(\pi-\theta) + \frac{1}{32ik}\{[48\alpha_{11} + 48\alpha_{12} + 32\alpha_{32} - 308\alpha_{33} - 60\alpha_{34} - 48\alpha_{54} + 638\alpha_{55} + 70\alpha_{56} - (32\sqrt{6})\alpha^2 + (48\sqrt{5})\alpha^4]\cos\theta + [420\alpha_{33} + 140\alpha_{34} + 112\alpha_{54} - 2772\alpha_{55} - 420\alpha_{56} - (112\sqrt{5})\alpha^4]\cos^3\theta + [-882\alpha_{54} + 2310\alpha_{55} + 462\alpha_{56}]\cos^5\theta\}. \tag{38}$$

TABLE VII. Summary of experimental data for phase shift analysis.

Observable	θ (degrees)	Experimental value	Reference
σ_{tot}	$\theta > 20$	22.24 ±0.70 mb	a
I_0	90	3.72 ±0.19 mb	b, c
I_0/I_0 (90°)	80.2	1.045±0.039	b, c
I_0/I_0 (90°)	71.4	0.971±0.032	b, c
I_0/I_0 (90°)	64.0	0.958±0.032	b, c
I_0/I_0 (90°)	60.8	1.013±0.041	b, c
I_0/I_0 (90°)	52.4	0.997±0.035	b, c
I_0/I_0 (90°)	44.8	1.008±0.026	b, c
I_0/I_0 (90°)	36.0	1.074±0.040	b, c
I_0/I_0 (90°)	31.9	1.031±0.031	b, c
I_0/I_0 (90°)	23.4	1.098±0.033	b, c
I_0/I_0 (90°)	18.6	1.024±0.078	d, e
I_0/I_0 (90°)	14.8	1.038±0.086	d, e
I_0/I_0 (90°)	11.3	0.935±0.108	d, e
I_0/I_0 (90°)	9.1	1.078±0.091	d, e
$P/\sin\theta\cos\theta$	76.2	0.613±0.108	f
$P/\sin\theta\cos\theta$	63.9	0.635±0.068	f
$P/\sin\theta\cos\theta$	53.4	0.633±0.052	f
$P/\sin\theta\cos\theta$	42.9	0.760±0.040	f
$P/\sin\theta\cos\theta$	32.3	0.837±0.060	f
$P/\sin\theta\cos\theta$	21.6	0.891±0.067	f
$1-D$	80.5	0.528±0.063	f
$1-D$	65.2	0.497±0.048	f
$1-D$	52.0	0.467±0.060	f
$1-D$	36.5	0.544±0.081	f
$1-D$	25.8	0.701±0.055	f
$1-D$	23.0	0.755±0.079	f
$R/\cos(\theta/2)$	80.1	0.752±0.114	f
$R/\cos(\theta/2)$	70.9	0.381±0.088	f
$R/\cos(\theta/2)$	54.1	0.322±0.058	f
$R/\cos(\theta/2)$	41.8	0.111±0.076	f
$R/\cos(\theta/2)$	34.4	−0.175±0.084	f
$R/\cos(\theta/2)$	22.3	−0.330±0.142	f
$A/\sin(\theta/2)$	76.3	0.382±0.078	g
$A/\sin(\theta/2)$	51.4	0.016±0.088	g
$A/\sin(\theta/2)$	25.4	−1.542±0.363	g

[a] See reference 1.
[b] Chamberlain, Segrè, and Wiegand, Phys. Rev. **83**, 923 (1951).
[c] O. Chamberlain and J. D. Garrison, Phys. Rev. **95**, 1349 (1954).
[d] Chamberlain, Pettengill, Segrè, and Wiegand, Phys. Rev. **93**, 1424 (1954); **95**, 1348 (1954).
[e] D. Fischer and Gerson Goldhaber, Phys. Rev. **95**, 1350 (1954).
[f] This work.
[g] James Simmons, Phys. Rev. **104**, 416 (1956).

At 310-Mev incident proton energy, the momentum of the proton in the center-of-mass system is $\mathbf{p} = \hbar\mathbf{k}$ where $|\mathbf{k}| = k = 1.933\times10^{13}$ cm^{-1}. The nonrelativistic Coulomb scattering amplitude is denoted by $f_C(\theta)$, where

$$f_C(\theta) = -\frac{n}{k(1-\cos\theta)}\exp\{-in\log[\tfrac{1}{2}(1-\cos\theta)]\}. \tag{39}$$

The observables I_0, P, D, R, and A may now be expressed as a function of the phase shifts through the use of Eqs. (31), (34)–(38). In all, we have available 36 measurements of the observables including 4 small-angle measurements of the differential cross section in the region where Coulomb interference effects are present. A summary of the experimental information is presented in Table VII.

The calculation of phase shifts which fit the data proceeded along the lines of the meson-nucleon phase shift calculation done by Fermi, Metropolis, and Alei.*

* Fermi, Metropolis, and Alei, Phys. Rev. **95**, 1581 (1954).

TABLE VIII. Phase shift solutions for which $\mathfrak{M}<60$.

Phase \ Solution	1 ($\mathfrak{M}=17.9$)	2 ($\mathfrak{M}=21.7$)	3 ($\mathfrak{M}=23.8$)	4 ($\mathfrak{M}=24.5$)
δ_0	$-10.1\pm2.5°$	$-19.5\pm2.0°$	$-10.9\pm2.5°$	$-27.0\pm2.0°$
δ_2	$13.8\pm0.7°$	$5.3\pm0.6°$	$14.2\pm0.8°$	$5.8\pm0.6°$
δ_4	$2.3°$	$2.6°$	$2.4°$	$2.4°$
δ_{10}	$-13.7\pm2.2°$	$-35.4\pm1.9°$	$-3.4\pm1.4°$	$-24.7\pm1.9°$
δ_{11}	$-26.0\pm1.3°$	$-11.1\pm1.0°$	$-19.1\pm0.8°$	$-6.6\pm1.0°$
δ_{12}	$16.8\pm1.0°$	$23.1\pm0.8°$	$23.3\pm0.7°$	$25.8\pm0.8°$
ϵ_2	$-3.8\pm2.1°$	$-23.1\pm1.6°$	$4.3\pm1.0°$	$-16.7\pm1.6°$
δ_{22}	$1.9\pm1.0°$	$-3.0\pm0.9°$	$-1.0\pm0.6°$	$-2.2\pm0.9°$
δ_{23}	$3.2\pm1.1°$	$1.4\pm0.4°$	$-1.4\pm0.6°$	$2.7\pm0.4°$
δ_{24}	$4.9\pm0.5°$	$5.1\pm0.8°$	$2.1\pm0.5°$	$4.0\pm0.8°$
ϵ_4	$-28.7°$	$-43.8°$	$-26.8°$	$-15.5°$
δ_{54}	$2.3°$	$2.1°$	$-0.1°$	$0.5°$
δ_{55}	$1.5°$	$0.1°$	$2.4°$	$0.6°$
δ_{56}	$2.8°$	$2.8°$	$0.9°$	$0.6°$

Phase \ Solution	5 ($\mathfrak{M}=34.2$)	6 ($\mathfrak{M}=34.6$)	7 ($\mathfrak{M}=41.3$)	8 ($\mathfrak{M}=52.3$)
δ_0	$47.2\pm1.9°$	$-0.3\pm2.3°$	$11.9\pm2.1°$	$28.6\pm2.6°$
δ_2	$1.8\pm0.5°$	$13.8\pm0.6°$	$0.6\pm0.9°$	$5.7\pm0.8°$
δ_4	$4.2°$	$0.3°$	$2.9°$	$1.0°$
δ_{10}	$38.1\pm1.9°$	$-64.1\pm1.9°$	$4.3\pm2.3°$	$67.6\pm3.4°$
δ_{11}	$5.6\pm0.9°$	$-12.8\pm0.9°$	$36.1\pm1.0°$	$10.1\pm1.1°$
δ_{12}	$7.8\pm0.4°$	$8.8\pm0.5°$	$4.6\pm0.4°$	$2.8\pm0.6°$
ϵ_2	$9.0\pm1.9°$	$-1.0\pm3.1°$	$-1.5\pm2.5°$	$-2.8\pm3.6°$
δ_{22}	$-14.3\pm1.1°$	$-1.0\pm0.7°$	$-11.9\pm0.9°$	$-7.6\pm0.8°$
δ_{23}	$-2.6\pm0.8°$	$4.2\pm1.1°$	$-4.6\pm0.7°$	$-6.3\pm0.8°$
δ_{24}	$4.4\pm0.3°$	$5.4\pm0.3°$	$3.6\pm0.3°$	$3.7\pm0.3°$
ϵ_4	$-45.4°$	$36.9°$	$-32.1°$	$-23.5°$
δ_{54}	$0.8°$	$2.7°$	$0.6°$	$2.0°$
δ_{55}	$1.0°$	$-0.5°$	$0.9°$	$1.7°$
δ_{56}	$2.0°$	$1.7°$	$2.0°$	$1.9°$

A random set of phase shifts was chosen and the quantity

$$\mathfrak{M}(\delta)=\sum_{i=1}^{36}\left(\frac{\Delta_i}{\epsilon_i}\right)^2 \tag{40}$$

was minimized by varying the phase shifts δ. In Eq. (40), Δ_i is the deviation of the calculated from the measured value of the ith observable and ϵ_i is the experimental error in the measurement. The bulk of the calculations were performed on the Los Alamos "MANIAC" electronic computer; however, the final phase of the work was completed on the Los Alamos "704" computer. A detailed discussion of the search procedures used to minimize $\mathfrak{M}(\delta)$ is contained in the accompanying paper.[32] In all, 420 random sets of phase shifts were taken as starting points for the calculation and these led to only 19 different solutions. Each solution was obtained at least 5 times from different random sets of starting points; thus we feel that the phase shift space has been adequately explored. The validity of the 19 solutions obtained was estimated by comparing the values of $\mathfrak{M}$ with the value expected from statistical considerations. The best four solutions have $\mathfrak{M}$ values between 17 and 25 and the next four solutions have $\mathfrak{M}$ values between 34 and 53. The remaining 11 solutions have $\mathfrak{M}>62$. If the true phase shifts for partial waves with $l>5$ are indeed negligible and if the errors on the measurements are normally distributed, then the most probable value of $\mathfrak{M}(=\mathfrak{M}_0)$ at the relative minimum, which lies in the neighborhood of the true solution, is the difference between the number of observables and the number of phase shifts. For our case $\mathfrak{M}_0=36-14=22$. The distribution law for the $\mathfrak{M}$ values is a Gaussian about $\mathfrak{M}_0$ with standard deviation $(2\mathfrak{M}_0)^{\frac{1}{2}}$; thus the probability that $14<\mathfrak{M}<34$ is 0.90. The probability that $\mathfrak{M}>34$ is approximately 0.05 and the probability that $\mathfrak{M}>40$ is approximately 0.01. Therefore, on the basis of statistical considerations we exclude from further considerations the 11 solutions with $\mathfrak{M}>62$. The remaining eight solutions are presented in Table VIII along with their $\mathfrak{M}$ values. The phase shifts listed include both Coulomb and nuclear effects. In the absence of nuclear forces they reduce to the Coulomb phase shifts Φ_l. Caution should be exercised in the interpretation of the mixing parameter ϵ_j because the Blatt and Biedenharn definition of this parameter[10] (i.e., the formulation used here) does not give a good indication of the degree to which l is conserved. The value of ϵ_j depends upon the phases of the basis vectors in terms of which the S matrix is defined. A detailed discussion of this point is contained in the appendix of reference 32.

The calculation of the errors in the phase shifts proceeded according to the method given by Anderson, Davidon, Glicksman, and Kruse.[33] Errors were not obtained for the G or H phase shifts or ϵ_4. It should be noted that the G and H phase shifts are uniformly small and may be taken as zero without appreciably altering the validity of the solution. These higher phase shifts were only inserted into the analysis in the last phase of the work in order to verify that the effect of higher waves was indeed negligible.

The eight sets of phase shifts listed in Table VIII are subject to additional restrictions imposed by the unitarity and symmetry of the complete S matrix for the p-p system. In the reaction $p+p\rightarrow\pi^++d$, we define transition amplitude phase angles relative to the production from an initial $^1D_2$ state of the two-proton system. These angles are τ_0 and τ_1 for initial $^1S_0$ and $^3P_1$ states, respectively. According to Gell-Mann and Watson,[34] τ_0 and τ_1 are related to the p-p phase shifts in

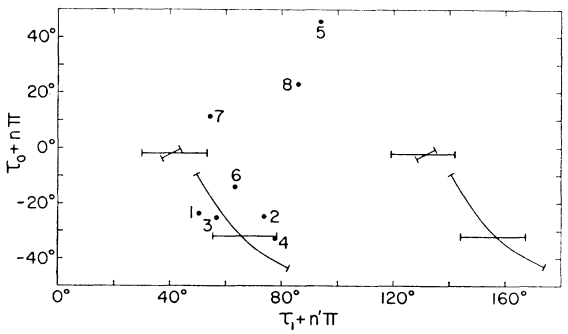

FIG. 10. The four possible sets of phase angles (τ_0,τ_1) which fit the experimental results in the reaction $p+p\rightarrow\pi^++d$. The numbers indicate the predictions of the eight sets of phase shifts listed in Table VIII.

[33] Anderson, Davidon, Glicksman, and Kruse, Phys. Rev. **100**, 279 (1955).

[34] M. Gell-Mann and K. M. Watson, *Annual Reviews of Nuclear Science* (Annual Reviews, Inc., Stanford, 1954), Vol. 4, p. 219.

the $^1S_0$, $^3P_1$, and $^1D_2$ states by

$$\tau_0=\delta_0-\delta_2+n\pi,$$
$$\tau_1=\delta_{11}-\delta_2+(n'+\tfrac{1}{2})\pi, \quad (41)$$

where n and n' are integers. The measurement by Tripp[35] on the $p+p\rightarrow\pi^++d$ reaction at 340 Mev combined with the measurements by Crawford and Stevenson[36] of the total and differential cross section for this reaction, using polarized and unpolarized incident proton beams, determine trigonometric functions of the phase angles τ_0 and τ_1. Two values of τ_0 are consistent with the measurements, and for each of these values two values of τ_1 are admissible. This results in four combinations of τ_0 and τ_1 which fit the experimental results. Each set of angles (τ_0,τ_1) corresponds to a point in a plot of τ_0 *versus* τ_1. These are exhibited in Fig. 10 along with their errors. From each of the 8 solutions of Table VIII, values of τ_0 and τ_1 may be calculated and these are also plotted in Fig. 10. It is seen that solutions 1, 2, 3, 4, and 6 are all compatible with the same combination of τ_0 and τ_1 whereas solutions 5, 7, and 8 are compatible with none of these combinations and hence must be discarded. The values of the phase angles, τ_0 and τ_1, which are compatible with our solutions 1, 2, 3, 4, and 6, require production of the π meson predominantly from an initial $^1D_2$ state rather than from the $^1S_0$ state. This provides additional evidence for the Fermi type $(\frac{3}{2},\frac{3}{2})$ π-p interaction.

The five solutions which fit all the presently available data have the following common features; (i) negative $^1S_0$ and positive $^1D_2$ phase shifts characteristic of a repulsive hard core surrounded by an attractive potential, (ii) negative $^3P_0$ and $^3P_1$ phases and positive $^3P_2$ phase shift which for weak interactions is characteristic of an $\mathbf{L}\cdot\mathbf{S}$ force; and (iii) small G and H phase shifts. A choice among these sets of phase shifts cannot be made with the presently available information; however, the measurement of the polarization correlation parameters[11,32] C_{nn} and C_{KP} could resolve the question. The predictions of the five solutions for this parameter at $\theta=90°$ are collected in Table IX. The dispersion of the values is large, and thus a single measurement near $\theta=90°$ should suffice to distinguish between the solutions.

TABLE IX. Polarization correlation at $\theta=90°$.

Solution	C_{nn}	C_{KP}
1	0.158	0.363
2	0.711	0.516
3	0.300	0.251
4	0.490	0.511
6	0.425	−0.358

The inclusion of the n-p cross section and polarization data into the phase shift analysis has not yet been attempted. A selection among the various solutions may conceivably be obtained by such an analysis if charge independence is assumed. Finally, it should be noted that the phase shift solutions obtained at this energy should join smoothly with solutions at lower energies. This condition may be valuable in any attempt to extend a particular one of the 310-Mev solutions into an energy region where the experimental information is not as extensive.

VI. ACKNOWLEDGMENTS

Assistance during the many days of cyclotron time has been generously provided by Dr. Gordon Pettengill, Dr. David Fischer, Dr. John Baldwin, and Dr. Robert E. Donaldson. Discussions of polarization theory with Dr. Lincoln Wolfenstein, Dr. Henry P. Stapp, and Dr. Burton Fried have been extremely valuable.

The authors wish to thank Mr. James Vale and the cyclotron crew for providing the necessary beams under sometimes difficult conditions.

[35] R. Tripp, Phys. Rev. **102**, 862 (1956).
[36] F. S. Crawford, Jr. and M. L. Stevenson, Phys. Rev. **97**, 1305 (1955).